



Universiteit
Leiden
The Netherlands

Evaluation of a radiological tool for semiautomatic scalar translocation detection after cochlear implantation

Arends, S.R.S.; Briaire, J.J.; Geiger, S.; Nauwelaers, T.; Frijns, J.H.M.

Citation

Arends, S. R. S., Briaire, J. J., Geiger, S., Nauwelaers, T., & Frijns, J. H. M. (2024). Evaluation of a radiological tool for semiautomatic scalar translocation detection after cochlear implantation. *Otology & Neurotology*, 45(4), e322-e327.
doi:10.1097/MAO.0000000000004161

Version: Publisher's Version
License: [Creative Commons CC BY 4.0 license](#)
Downloaded from: <https://hdl.handle.net/1887/4197473>

Note: To cite this publication please use the final published version (if applicable).

OPEN

Evaluation of a Radiological Tool for Semiautomatic Scalar Translocation Detection After Cochlear Implantation

*Sebastiaan R.S. Arends, *Jeroen J. Briaire, †Stephan Geiger,
†Tim Nauwelaers, and *‡Johan H.M. Frijns

*Department of Otorhinolaryngology and Head & Neck Surgery, Leiden University Medical Center, Leiden, the Netherlands; †Advanced Bionics, European Research Center, Hannover, Germany; and ‡Leiden Institute for Brain and Cognition, Leiden University, Leiden, the Netherlands

Objective: To evaluate the clinical applicability of a semiautomatic radiological tool for scalar translocation detection.

Study Design: Retrospective study.

Setting: Tertiary care academic center.

Patients: We included 104 patients implanted with 116 HiFocus Mid-Scala electrode arrays between January 2013 and September 2016.

Intervention: Cochlear implantation.

Main Outcome Measures: The tool's scalar position assessments were compared with manual ones by calculating intraclass coefficient (ICC) for individual contacts and sensitivity and specificity for translocation detection of the whole array. In addition, ICC was calculated for diameters A and B, ratio A/B, and angular insertion depth (AID).

Results: Nine-one percent of cases could be processed, which took 5 to 10 minutes per case. Comparison of manual and

semiautomatic scalar position showed for individual contacts an ICC of 0.89 and for the whole array a sensitivity of 97% and a specificity of 96%. ICCs for A, B, and A/B were 0.82, 0.74, and 0.39 respectively. For AID, ICC of each of the 16 contacts was 0.95 or higher.

Conclusions: The semiautomatic radiological tool could analyze most cases and showed good to excellent agreement with manual assessments for translocation detection, diameter A, diameter B, and AID. The variability between semiautomatic and manual measurements is comparable to interobserver variability, indicating that clinical implementation of the tool is feasible.

Key Words: Cochlear implantation—Computed tomography—Scalar translocation—Semiautomatic.

Otol Neurotol 45:e322–e327, 2024.

INTRODUCTION

Cochlear implantation (CI) is an established treatment for restoring hearing in individuals with severe to profound sensorineural hearing loss. Although most CI recipients experience significant improvement in speech recognition, a large variation in outcomes is observed (1). An important, potentially modifiable, factor influencing the postoperative outcome is scalar translocation (2–6). This is a common complication of CI surgery where the electrode array dislocates from scala tympani (ST) to scala vestibuli (SV).

A systematic review including more than 2,000 patients found the occurrence of scalar translocation to be 32% for precurved electrode arrays and 7% for straight electrode arrays (7).

The mechanism underlying the detrimental effects of translocation on hearing outcomes is believed to involve two main factors (8). First, the migration of the electrode array results in damage to the basilar membrane (BM) and/or osseous spiral lamina, which compromises any remaining hearing ability and triggers an inflammatory response. Second, translocation causes damage to the spiral ganglion cells and suboptimal positioning of the electrode array for stimulating the spiral ganglion cells. The malpositioned part of the electrode array in SV can be situated in such close proximity to the modiolus of the adjacent cochlear turn that cross-turn stimulation may occur. Moreover, precurved arrays are positioned near the lateral wall during translocation (in contrast to the intended modiolar wall position), resulting in a greater distance from the spiral ganglion cells and hence less precise stimulation. Examples of an electrode array fully inserted in ST and one with a translocation are displayed in Figure 1.

Address correspondence and reprint requests to Jeroen J. Briaire, Ph.D., at Leiden University Medical Center, Department of Otorhinolaryngology, PO Box 9600, 2300 RC Leiden, The Netherlands; E-mail: J.J.Briaire@lumc.nl

Sources of support and disclosure of funding: S.G. and T.N. are employees of Advanced Bionics. S.A., J.B., and J.F. declare no conflicts of interest.

This is an open access article distributed under the Creative Commons Attribution License 4.0 (CCBY), which permits unrestricted use, distribution, and reproduction in any medium, provided the original work is properly cited.

DOI: 10.1097/MAO.0000000000004161

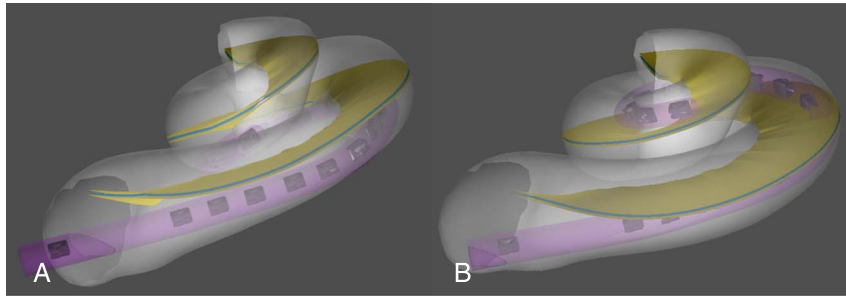


FIG. 1. Examples of three-dimensional cochlea and electrode array models generated by the radiological tool. *A*, An array positioned fully in scala tympani as intended. *B*, An array with translocation to scala vestibuli.

As it is one of the precursors for inferior outcomes, prevention of scalar translocation has become an important goal in CI research. Various technologies have been proposed to achieve this objective, including preoperative planning tools based on imaging (9), intraoperative impedance measurements (10), and robot-assisted electrode array insertion (11). Nevertheless, accurate postoperative diagnosis remains necessary to serve as a reference for new technologies. In addition, simply providing the surgeon with feedback of translocation shortly after the surgery has been shown to reduce the rate of translocation (6,12).

The criterion standard for diagnosis of scalar translocation is histopathology, but because this is not possible in vivo, computed tomography (CT) is considered the criterion standard in a clinical setting, using either conventional CT or cone beam CT (8). However, manual determination of scalar translocation from CT is time-consuming and prone to intraobserver and interobserver variability (13,14). Therefore, (semi)automatic analysis of CT images would be a preferred method for detection of scalar translocation from CT images, with the added benefit of being able to provide more detailed information than manual determination. A study by Sismono et al. (15) found that semiautomatic determination of scalar translocation on cone beam CT images was in full agreement with the opinion of two experienced radiologists in 23 cases, demonstrating that this is a feasible approach. Recently, a semiautomatic radiological tool has been developed that can, among others, detect translocation (16). The aim of this study was to evaluate the clinical applicability of this tool by comparing its scalar position assessments to a previously validated manual method (14) using a large set of preoperative and postoperative CT images from clinical practice.

MATERIALS AND METHODS

Patient Population

To evaluate the radiological tool, we used an existing dataset of 152 patients implanted with a total of 168 HiFocus Mid-Scala (MS) and HiFocus 1J electrode arrays (Advanced Bionics, Valencia, CA). However, because the radiological tool currently does not support 1J implants, only patients implanted with an MS array were included in this study. This group consists of 104 patients with a total of 116 implanted ears. All patients were implanted between January 2013 and September 2016 in the Leiden University Medical

Center. The MS electrode is a precurved array, containing 16 stimulating electrode contacts and one nonstimulating marker. Table 1 summarizes demographic characteristics of the patient population. The prevalence of translocation in the study population is higher than the prevalence of translocation for all patients implanted in our center, as a result of selecting a subset of the existing dataset that contains a large number of translocated arrays to evaluate the semiautomatic tool's accuracy (6).

Radiological Evaluation

Each patient underwent two multislice CT examinations (Aquilion; Toshiba Medical Systems, Otawara, Japan) with an isotropic acquisition voxel size of 0.45 or 0.50 mm. The first scan was made before the surgery and the second a day after the surgery, as part of the standard clinical workflow in our institution. From these scans, multiplanar reconstructions were made in which a plane goes through the basal turn of the cochlea. The preoperative and postoperative scans were aligned using manually selected anatomical landmarks from the cochlea coordinate system (17). On the preoperative scan, the largest distance from round window to the lateral wall (diameter A) and the distance perpendicular to it (diameter B) were measured (18). Ratio A/B, describing the shape of the cochlea, was obtained by dividing diameter A by diameter B. Then, electrode contacts were manually located on the postoperative scan, from which the angular insertion depth (AID) was calculated following the consensus coordinate system (17,19). Using the spatially synchronized scans and electrode positions, midmodiolar sections of each of the 16 electrode contacts were presented side by side in random order to an experienced head and neck radiologist for evaluation of the scalar position of that electrode contact (20). For each electrode contact, the radiologist assigned a score ranging from 0 to 5: 0, contact could

TABLE 1. Demographic characteristics of patient population

	n = 104 Patients, n = 116 Ears
Age at implantation, mean \pm SD, yr ^a	47.8 \pm 25.9
Female, n (%) ^a	57 (54.8)
Right-sided, n (%)	54 (46.6%)
AID, mean \pm SD, deg	416 \pm 36
Translocation, n (%)	39 (33.6)

^aCalculated over individual patients instead of ears.

AID indicates angular insertion depth; SD, standard deviation.

not be assessed; 1, certain ST position; 2, likely ST position; 3, intermediate position; 4, likely SV position; and 5, certain SV position (14,21,22). The electrode array as a whole was considered to be translocated if a total of two or more individual contacts were assessed to be located in SV (i.e., a score of 4 or 5). Because the radiological tool uses a different scale for scoring the scalar position (see discussion hereinafter), the manual scores were converted from the original five-point scale to the tool's three-point scale. Certain and likely ST assessments were joined as ST assessments, and certain and likely SV assessments were joined as SV assessments. The electrode closest to the basal end that was located in SV was considered to be the position of the translocation.

Radiological Tool

We used a research version of the radiological tool, as it is not yet available commercially. As described by Geiger et al. (16), it uses three-dimensional (3D) models of cochlea, BM, and the electrode array for surgical planning and postoperative assessment of the electrode position, including the scalar position of the electrode contacts. It currently supports postoperative assessment of patients implanted with MS or SlimJ electrode arrays. The cochlea and BM models are obtained by fitting an active shape model to the preoperative scan, based on four manually placed anatomical landmarks (23). Automatic localization of electrode contacts is used to fit an electrode array model to the postoperative scan. The preoperative and postoperative scans are spatially synchronized to be able to compare the electrode position relative to the cochlea and BM. Before placing the four anatomical landmarks, the user first has to crop the scan and align it to the plane through the basal turn of the cochlea. These steps are depicted in Figure 2. We used the cochlea 3D model to extract diameters A and B, as these are not directly measured by the tool. Note that diameters A and B were measured using a different method than the original definition by Escudé et al. (18), where A starts at the center of the round window and both lines go through the modiolar axis. Because the modiolar axis and center of the round window marker are not retained in the tool's output, satisfying these requirements was not possible. Instead, diameter A was measured as the distance between the beginning of the model (at the basal end of the round window) and a point on the lateral wall as far away as possible. Diameter B was measured as

the distance between two points on the lateral wall, placed so that the line connecting them is perpendicular to A and as large as possible. Ratio A/B was computed from diameters A and B. The AID and scalar location of each contact were extracted from the report that is generated by the tool upon analysis of the spatially synchronized cochlea, BM, and electrode array models. The scalar location is rated as a score ranging from 0 to 2: 0, ST position; 1, intermediate position; and 2, SV position.

Statistical Analysis

The cases where analysis was not possible using the radiological tool were compared with the cases where analysis was possible to identify differences between these groups. For the cases where analysis was possible, diameters A and B, ratio A/B, AID, and scalar location of individual contacts were evaluated for their correlation to manual assessments. Because these are considered repeated measurements by two fixed observers (manually and using the radiological tool), intraclass correlation coefficient (ICC) with 95% confidence interval was calculated using a two-way mixed-effects model for consistency, using single measurements for reliability. ICC is interpreted as poor (0.00–0.39), fair (0.40–0.59), good (0.60–0.74), or excellent (0.75–1.00) (24). Determining the presence of scalar translocation for the whole array is considered a binary diagnostic test and was evaluated by calculating sensitivity and specificity. *t* Tests and χ^2 tests were used to compare means and proportions, respectively. A *p* value of 0.05 or less was considered statistically significant. When considering statistical significance of outcomes for each of the 16 electrode contacts separately, Bonferroni correction was applied. Statistical analysis was performed using R statistical software (version 4.2.1, <https://www.r-project.org/>).

RESULTS

Of the 116 cases, 97 could be analyzed on the first try, 9 took more than one attempt of placing manual landmarks before analysis was possible, and 10 cases could not be fully analyzed despite repeated attempts. In all of these 10 cases, preoperative analysis was possible, but postoperative analysis was not, which often turned out to be caused by the electrode localization algorithm finding too many or too few electrode contacts. Mean AID of the 10 cases that could not be analyzed was significantly deeper than for

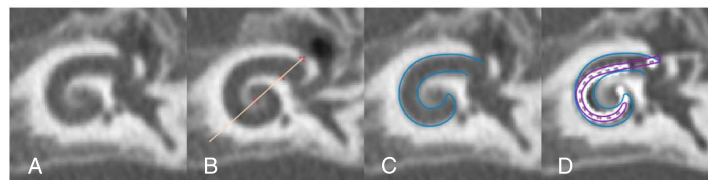


FIG. 2. Analysis steps using the radiological tool. A, Crop and realign CT to cochlear view. B, Place anatomical landmarks, C, Generate cochlea 3D model; D, Generate electrode model from spatially synchronized postoperative CT indicates computed tomography.

the cases where analysis was successful (459 versus 412 degrees, $p = 0.001$). Other patient characteristics did not differ significantly between these groups. The following results are for the 106 cases where semiautomatic analysis was possible. Although the time required was not measured in a systematic manner, it took 5 to 10 minutes on average to analyze one case.

Measurements of diameters A and B, ratio A/B, and the AID are depicted in Figure 3. Semiautomatic measurement resulted in systematically larger diameters than manual measurements for both A (mean, 9.54 versus 8.89 mm; $p < 0.001$) and B (mean, 7.15 versus 6.69 mm; $p < 0.001$). Mean absolute differences for A and B were 0.65 and 0.47 mm, respectively. Diameter A shows excellent correlation to manual measurements with an ICC of 0.82 (0.75–0.88), whereas B shows good correlation with an ICC of 0.74 (0.64–0.81). Mean ratio A/B was 1.33 for both manual and semiautomatic measurements, with a mean absolute difference of 0.04, but showed poor ICC of 0.39 (0.21–0.54). Manual measurements for ratio A/B were between 1.22 and 1.45, whereas semiautomatic measurements were within a narrower range between 1.26 and 1.38.

Upon analysis of AID, we noticed that measurements by the radiological tool included three outliers, where the AID for one contact seemed to be measured as if it were located in the next turn (i.e., the value was approximately 360

degrees higher than expected based on the AID of adjacent contacts). To prevent a disproportionate influence of these values, they were corrected by subtracting 360 degrees. The mean absolute difference in AID from semiautomatic versus manual determination was 8.7 degrees, which is far less than the mean difference of 25.6 degrees between consecutive contacts according to manual measurements. ICC was excellent for AID of each of the 16 contacts separately (range, 0.95–0.98). For the AID of the most apical contact, often referred to as insertion depth of the electrode as a whole, ICC was 0.95 and the mean absolute difference was 15.4 degrees. The mean difference in AID between the two most apical contacts as measured manually was 49.8 degrees.

ICC of semiautomatic and manual scalar location for individual contacts was 0.89 (0.88–0.90). After combining these individual scores into translocation of the entire electrode array, comparison of semiautomatic scores to the manual scores, shown in Table 2, resulted in sensitivity of 97% and specificity of 96%. For those cases in which both methods rated the array as translocated, the average difference in position of translocation was 0.6 contacts.

DISCUSSION

Accurate postoperative diagnosis of scalar translocation in cochlear implant recipients is a relevant, yet challenging

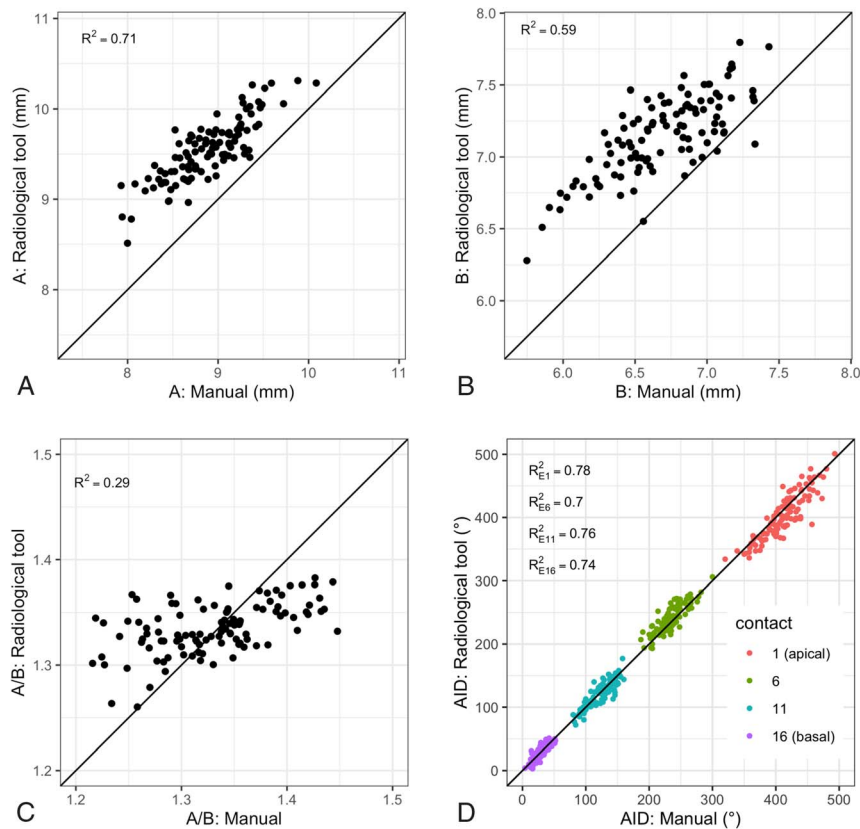


FIG. 3. Scatterplots of manual measurements compared with measurements from the radiological tool. The diagonal lines represent perfect agreement between measurements. Diameter A (A), diameter B (B), ratio A/B (C), and angular insertion depth in degrees (D) from the round window (only contacts 1, 6, 11, and 16 are displayed for clarity, but the patterns for other contacts are similar).

TABLE 2. Radiological tool assessments of translocation compared with manual assessments

		Manual Assessment	
		Translocation	No Translocation
Radiological tool	Translocation	34	3
	No translocation	1	68

task. This study set out to evaluate a radiological tool for semiautomatic analysis of the electrode location from CT images. The tool creates a 3D model of the cochlea and the BM based on the preoperative scan, and adapts a spatially synchronized 3D model of the electrode array based on the postoperative scan. A large majority of cases can be analyzed quickly using this tool. Measurements of A, B, and AID demonstrate good to excellent correlation to manual measurements, whereas measurements of ratio A/B show poor correlation. Most notably, scalar position shows excellent agreement with the opinion of an experienced radiologist, with an ICC of 0.89 for individual contacts and sensitivity of 97% and specificity of 96% for detecting translocation in the complete electrode array. We found that the tool could fully analyze 91% of the cases, with the full process of cropping and aligning the scan, placing landmarks and analysis taking roughly 5 to 10 minutes. This would make implementation into a clinical workflow feasible. However, a serious drawback is that the tool is limited to postoperative analysis of electrode arrays from one manufacturer only. Ideally, this kind of tool should be applicable to every cochlear implant recipient, ensuring a standardized assessment between patients. Further standardization could be attained by automating the process entirely, removing any interobserver variability.

Diameters A and B were introduced by Escudé et al. (18) as a simple way to define cochlear size. They are also used to estimate cochlear duct length, predict AID (25), and consequently select an appropriate electrode array. Rivas et al. (26) developed an algorithm that automatically measures A and compared it with the manual measurements of two expert observers. The mean absolute differences between expert measurements and between automatic measurements and both of the experts separately were 0.18, 0.25, and 0.18 mm, respectively. In another study, a tool similar to the one we used was evaluated by measuring intraobserver and interobserver variability of experts using the tool (27). They found mean absolute differences between and within observers, respectively, of 0.96 and 0.29 mm for A and 0.34 and 0.30 mm for B. Compared with these results, our absolute mean differences between manual and semiautomatic measurements of 0.65 mm for A and 0.48 mm for B are relatively large. However, ICC is good to excellent, comparable to the interobserver ICC between two experts reported by Oh et al. (28). The systematic overestimation of the diameters by the radiological tool can (at least partially) be explained by the approach we used to measure the diameters. Because the markers indicating the center of the round window and the modiolar axis are not retained in the tool's output, we used the basal end instead of the center of the round

window to measure A and could not check the requirement that both lines cross the modiolar axis. Another possible explanation is that a manual measurement is carried out on one slice of the CT, whereas the algorithm we used to find the longest distance considers the full 3D cochlea model, perhaps resulting in a slightly larger result than is possible when considering only one slice.

An interesting finding in our study is that, despite good to excellent correlation for diameters A and B separately, correlation for ratio A/B is poor. We hypothesized that this could be a result of the systematic measurement errors of diameters A and B discussed previously. However, subtracting the absolute or relative mean systematic error from the tool's measurements before calculating ratio A/B did not lead to meaningful changes in the results. We also observed that values for ratio A/B as measured by the radiological tool fall within a much narrower range than values measured manually. Because diameters A and B are extracted from the 3D cochlea models that are generated using an active shape model, and ratio A/B is a measure describing the shape of the cochlea, the narrow range of values may be a reflection of too strict constraints on the shape of the cochlea model. Thus, to improve the active shape model's accuracy in representing cochlear anatomy, it seems that increasing the variability of ratio A/B should be a priority. To the best of our knowledge, no previous studies have evaluated intraobserver or interobserver variability for ratio A/B that we can compare our results to.

The AID indicates how deep each electrode contact is located within the cochlea, which may be used for patient-specific frequency mapping in the speech processor. Canfarotta et al. (9) reported intraobserver and interobserver ICCs of 0.99 and 0.98 and mean absolute difference of 9.9 degrees for the most apical contact as measured using a tablet-based tool similar to the one we used. In their study, they only examined patients implanted with a lateral wall array. Because the contacts of a lateral wall array are located further away from the modiolar axis, a certain absolute localization difference will lead to a smaller difference in AID compared with precurved arrays. For example, one study found an interobserver ICC of 0.96 for manual AID measurement of straight arrays (28), whereas another found an ICC of 0.67 for patients implanted with a precurved array (13). Our results show that the tool leads to consistent AID measurements that are comparable to manual measurements.

Our main interest in this study was the reliability of scalar position assessments. We found that the tool produces judgments of the scalar position that closely correspond to the opinion of an expert radiologist, both for individual contacts and the complete electrode array. In a previous study from our group, reliability of manual scalar position determination for individual contacts was investigated (14). It showed intraobserver and interobserver ICCs of 0.86 and 0.83. These results are, however, not directly comparable to the current study, because scalar position was compared on a five-point scale, instead of the three-point scale we used in this study. For scalar translocation detection of the complete electrode array, Jia et al. (29) reported agreement between expert judgments on intraoperative cone

beam CT to be as low as 43 to 53%. Farnsworth et al. (13) found Cohen's κ of 0.78 for translocation agreement between experts in a relatively small study with three translocations in 34 patients. This means that differences between manual and semiautomatic scalar position assessments in our study are not necessarily errors from the tools, but could also be due to interobserver variability. To establish the true error rate of the tool's assessments, other judgments should be used for comparison, such as expert judgment from histology or high-quality images like micro-CT. In addition, intraobserver and interobserver variability will likely also be present in the assessments of the radiological tool, because it depends on the manual placement of anatomical landmarks. Sismono et al. (15) did observe perfect agreement between semiautomatic electrode localization approach and expert scalar position judgments on cone beam CT. However, this was a smaller study with only 23 patients with straight electrodes.

Although this study is relatively large, there are also some limitations. First, we included only patients implanted with a precurved array, and therefore, the results cannot directly be generalized to all array types. Although translocation detection is most relevant for precurved arrays because of the higher incidence, further research is required in patients implanted with straight arrays. In addition, we used images from one center with comparable voxel size and image quality. Any influence of these factors on the results thus remains unknown. Finally, we only evaluated the tool compared with manual measurements. Further examination of intraobserver and interobserver variability of using the tool would provide valuable information about the reliability of the tool measurements.

In this study, we evaluated a semiautomatic radiological tool for scalar translocation detection and other measures. It showed good to excellent correlation with manual assessments in 106 ears. The tool can quickly analyze most cases and is potentially applicable in clinical practice to provide reliable feedback after CI for a selection of patients.

REFERENCES

- Naples JG, Ruckenstein MJ. Cochlear implant. *Otolaryngol Clin North Am* 2020;53:87–102.
- Holden LK, Finley CC, Firszt JB, et al. Factors affecting open-set word recognition in adults with cochlear implants. *Ear Hear* 2013;34:342–60.
- O'Connell BP, Cakir A, Hunter JB, et al. Electrode location and angular insertion depth are predictors of audiologic outcomes in cochlear implantation. *Otol Neurotol* 2016;37:1016–23.
- Chakravorti S, Noble JH, Gifford RH, et al. Further evidence of the relationship between cochlear implant electrode positioning and hearing outcomes. *Otol Neurotol* 2019;40:617–24.
- Jwair S, Prins A, Wegner I, et al. Scalar translocation comparison between lateral wall and perimodiolar cochlear implant arrays—a meta-analysis. *Laryngoscope* 2021;131:1358–68.
- Van Der Jagt AMA, Briaire JJ, Boehringer S, Verbist BM, Frijns JHM. Prolonged insertion time reduces translocation rate of a precurved electrode array in cochlear implantation. *Otol Neurotol* 2022;43:E427–34.
- Dhanasingh A, Jolly C. Review on cochlear implant electrode array tip fold-over and scalar deviation. *J Otol* 2019;14:94–100.
- Munhall CC, Noble JH, Dawant B, Labadie RF. Cochlear implant translocation: Diagnosis, prevention, and clinical implications. *Curr Otorhinolaryngol Rep*. Published online December 1, 2022. doi:10.1007/s40136-022-00434-1.
- Canfarotta MW, Dillon MT, Buss E, et al. Validating a new tablet-based tool in the determination of cochlear implant angular insertion depth. *Otol Neurotol* 2019;40:1006–10.
- Dong Y, Briaire JJ, Siebrecht M, Stronks HC, Frijns JHM. Detection of translocation of cochlear implant electrode arrays by Intracochlear impedance measurements. *Ear Hear* 2021;42:1397–404.
- Daoudi H, Lahlou G, Torres R, et al. Robot-assisted cochlear implant electrode array insertion in adults: A comparative study with manual insertion. *Otol Neurotol* 2021;42:e438–44.
- Aschendorff A, Kromeier J, Klenzner T, Laszig R. Quality control after insertion of the nucleus contour and contour advance electrode in adults. *Ear Hear* 2007;28:75S–9S.
- Farnsworth PJ, Benson JC, Nassiri AM, et al. Improved cochlear implant electrode localization using coregistration of pre- and postoperative CT. *J Neuroimaging* Published online February 22, 2023. doi:10.1111/jon.13094.
- Van Der Jagt MA, Briaire JJ, Boehringer S, Verbist BM, Frijns JHM. Improved cochlear implant position with spatially synchronized pre- and post-operative midmodiolar cross-section CT and MR images. The cochlea depicted [doctoral thesis]. Published online 2021:81–95. Available at: <https://hdl.handle.net/1887/3238993>. Accessed January 7, 2022.
- Sismono F, Leblans M, Mancini L, et al. 3D-localisation of cochlear implant electrode contacts in relation to anatomical structures from in vivo cone-beam computed tomography. *Hear Res* 2022;426:108537.
- Geiger S, Iso-Mustajärvi M, Nauwelaers T, et al. Automatic electrode scalar location assessment after cochlear implantation using a novel imaging software. *Sci Rep* 2023;13:12416.
- Verbist BM, Skinner MW, Cohen LT, et al. Consensus panel on a cochlear coordinate system applicable in histologic, physiologic, and radiologic studies of the human cochlea. *Otol Neurotol* 2010;31:722–30.
- Escudé B, James C, Deguine O, et al. The size of the cochlea and predictions of insertion depth angles for cochlear implant electrodes. *Audiol Neurootol* 2006;11(suppl. 1):27–33.
- Van Der Marel KS, Briaire JJ, Wolterbeek R, Verbist BM, Frijns JHM. Development of insertion models predicting cochlear implant electrode position. *Ear Hear* 2016;37:473–82.
- Jagt AMAV, Kalkman RK, Briaire JJ, Verbist BM, Frijns JHM. Variations in cochlear duct shape revealed on clinical CT images with an automatic tracing method. *Sci Rep* 2017;7:17566.
- Helbig S, Mack M, Schell B, et al. Scalar localization by computed tomography of cochlear implant electrode carriers designed for deep insertion. *Otol Neurotol* 2012;33:745–50.
- Connor SEJ, Holland NJ, Agger A, et al. Round window electrode insertion potentiates retention in the scala tympani. *Acta Otolaryngol* 2012;132:932–7.
- Cootes TF, Taylor CJ, Cooper DH, Graham J. Active shape models—their training and application. *Comput Vision Image Understand* 1995; 61:38–59.
- Cicchetti DV. Guidelines, criteria, and rules of thumb for evaluating normed and standardized assessment instruments in psychology. *Psychol Assess* 1994;6:284–90.
- Müller-Graff FT, Voelker J, Kurz A, et al. Accuracy of radiological prediction of electrode position with otological planning software and implications of high-resolution imaging. *Cochlear Implants Int* 2023;24:144–54.
- Rivas A, Cakir A, Hunter JB, et al. Automatic cochlear duct length estimation for selection of cochlear implant electrode arrays. *Otol Neurotol* 2017;38:339–46.
- Cooperman SP, Aaron KA, Fouad A, et al. Assessment of inter- and intra-rater reliability of tablet-based software to measure cochlear duct length. *Otol Neurotol* 2021;42:558–65.
- Oh J, Cheon JE, Park J, et al. Cochlear duct length and cochlear distance on preoperative CT: Imaging markers for estimating insertion depth angle of cochlear implant electrode. *Eur Radiol* 2021;31:1260–7.
- Jia H, Torres R, Nguyen Y, et al. Intraoperative conebeam CT for assessment of intracochlear positioning of electrode arrays in adult recipients of cochlear implants. *AJNR Am J Neuroradiol* 2018;39:768–74.